

# The electro production of $d^*$ dibaryon

Di Qing<sup>1,2</sup>, He-ming Sun<sup>1</sup>, and Fan Wang<sup>1</sup>

<sup>1</sup>*Department of Physics, Nanjing University, Nanjing, 210093, China*

<sup>2</sup>*Institute of Modern Physics, Southwest Jiaotong University, Chengdu, 610031, China*

$d^*$  dibaryon study is a critical test of hadron interaction models. The electro production cross sections of  $ed \rightarrow ed^*$  have been calculated based on the meson exchange current model and the cross section around 30 degree of 1 GeV electron in the laboratory frame is about 10 nb. The implication of this result for the  $d^*$  dibaryon search has been discussed.

14.20.Pt, 21.30.Fe, 25.30.Dh, 25.30.Rw

## I. INTRODUCTION

The fundamental blocks of strong interaction have been confirmed to be quark and gluon. Meson, baryon, nucleus, and neutron star are the observed samples of the strong interaction matter. Theoretically it is expected that there should be other samples of the strong interaction matter such as exotic quark-gluon systems, strangelet, strange star, and quark-gluon plasma. Experimental search for these new strong interaction matters has been undertaken for two decades, even though there are some candidates of these new strong interaction matters but nothing new has been established. New facilities have been under operation or under construction for further experimental search. To help these search projects, new theoretical input is needed. An estimate of the  $d^*$  production cross section through the  $\pi d \rightarrow \pi d^*$  aimed to use the LAMPF  $\pi$  beam was reported in 1989 [1]. A strong production of  $d^*$ , aimed to use the existed proton machine, has been reported by Wong [2]. Intensive electron beam facilities in the GeV energy range are available. This paper reports an electro-production calculation of  $d^*$  ( $IJ^P = 03^+$ ) [1,3].

There are experimental indications of dibaryon states. A high mass ( $\sim 2.7$  GeV) dibaryon was reported by the Sacle group [4] and a low mass (2.06 GeV) one was reported by Moscow-Tuebingen group [5] in addition to other more tentative ones. H particle [6] has been hunted for more than 20 years. Why is  $d^*$  interesting?

Dibaryon states are closely related to the hadronic interaction, which is too complicated to be studied directly from the fundamental strong interaction theory, the QCD at present. Many QCD inspired models have been developed to describe the hadronic interaction.

The meson exchange model, based on meson-baryon coupling, was developed long before QCD [7] and it is still best at fitting the experimental data quantitatively [8]. However its validity in QCD is not clear at the moment. Moreover there are many phenomenological parameters fixed in the fitting process and in turn it is hard to make definite predictions for new physics such as the dibaryon states [9].

Chiral perturbation effective field theory [10] employs Goldstone bosons, resulting from spontaneous chiral symmetry breaking, as the effective degree of freedom in the low energy region, and the extension to the N-N interaction is encouraging [11]. Dibaryon has not been studied in this approach yet.

L.Ya. Glozman, D.O. Riska and G.E. Brown [12] proposed that the Goldstone boson is not only an effective degree of freedom for describing hadronic interactions but also good for analyzing baryon internal structure. In their model, constituent quarks and Goldstone bosons are used as the effective degrees of freedom. Up to now the application is mainly restricted in the baryon spectroscopy except a study on the origin of the N-N repulsive core.

A. Manohar and H. Georgi [13], however, have argued that between the chiral symmetry breaking scale ( $\sim 1$  GeV) and the confinement scale ( $\sim 0.2$  GeV), the effective degrees of freedom are Goldstone bosons, constituent quarks and gluons. Such a hybrid quark-gluon-meson exchange model has been developed to describe nucleon-baryon interactions and a semi-quantitative fit has been obtained [14]. Some dibaryon states have been studied with this model [15].

A constituent quark and effective one gluon exchange model [16] describes hadron spectroscopy quite well [17], but only the repulsive core of the N-N interaction was obtained when this model was extended to study hadron interactions [18].

The MIT bag model uses the current quark and gluon to describe hadron internal structure [19]. It was used extensively in the study of dibaryon states in the early 1980's and resulted in an explosion of dibaryon states [20]. It was realized latter that the unphysical boundary condition should be modified [21]. One modified version is the R-matrix method [22] and the other one is the compound quark model approach [23].

The Skyrme model [24] has also been used to study hadron interactions [25] and dibaryons [26]. Additional models might exist that should be added to the list.

It seems hard to discriminate these models just by the hadron spectroscopy and the existed scattering data of hadron interactions. Theoretically it is also hard to justify which effective degrees of freedom are the proper ones. On the other hand the well known phenomena, that the nucleus is a collection of nucleons rather than quarks, and that the nuclear force has similarities to the molecular force except for energy and length scale differences, have not been explained by any of these model approaches.

A pure quark-gluon model description of the  $N$ - $N$  interaction has been developed [3,27]. It starts from a multiquark system and demonstrates that in the  $N$ - $N$  channels, it is energetically favorable for the system to cluster into two nucleons and that the nuclear intermediate range attraction is caused by quark delocalization similar to the electron delocalization which induces intermediate range molecular attraction. In the 9 and 12 quark systems with quantum numbers of  ${}^3H$ ,  ${}^3He$  and  ${}^4He$  the nucleon clustering has been verified as well as the two nucleon system [28]. This model has been extended to  $N$ - $\Lambda$  and  $N$ - $\Sigma$  interactions [29] and the results show that the quarks delocalize properly in different channels to induce qualitatively correct  $N$ - $N$  (JI = 10, 01, 11, 00),  $N$ - $\Lambda$  (JI =  $1\frac{1}{2}$ ,  $0\frac{1}{2}$ ), and  $N$ - $\Sigma$  (JI =  $1\frac{1}{2}$ ,  $0\frac{1}{2}$ ,  $1\frac{3}{2}$ ,  $0\frac{3}{2}$ ) interactions. For other channels [3], such as  $\Delta\Delta$  (JI = 30),  $\Delta\Omega(3\frac{3}{2})$ ,  $\Delta\Sigma^*(3\frac{1}{2})$  and  $\Delta\Xi^*(31)$ , it is energetically favorable for the quarks to merge into quark matter instead of two baryons, and there are often strong effective attractions in these channels. In the  $\Delta\Delta$  (JI = 30), the  $d^*$  channel, the effective attraction is so strong that the total energy of the system ( $\sim 2.1$  GeV) is near the  $NN\pi$  threshold; therefore the  $d^*$  (JI = 30) might be a narrow resonance state [2].

Different model approaches give quite different mass of  $d^*$ . The meson baryon coupling model [9] gave a  $\Delta - \Delta$  binding of 11 – 340 MeV depending on the coupling constants of  $\rho$  and  $\omega$  and the hard core radii (0.2 – 0.3 fm). If the hard core radii are larger than 0.38 – 0.40 fm, the binding energy will be less than 10 MeV. The quark-meson-gluon hybrid model obtained a binding between 37 MeV and 80 MeV [30]. The pure gluon exchange model got 18 MeV binding even though there is a repulsive core in many other baryon-baryon channels [31]. MIT bag model will give a  $d^*$  mass of 2340 MeV if the bag radius is adjusted to give the minimum. On the other hand the R-matrix version of the modified bag model give a mass as high as 2840 MeV [22]. The skyrmion model obtained a very weak binding  $\sim 10$  MeV [32]. Therefore  $d^*$  study will provide a critical test of hadron interaction models. (This was already pointed out in the US Long Range Plan for Nuclear Science in 1996 [33].)

Quark delocalization plays a vital role in lowering the  $d^*$  mass. In a variational calculation this is nothing else but just a method to enlarge the variational Hilbert space. Therefore it might be a general property of quantum mechanics. If it is really realized in the nucleus (nucleon swollen explanation of the EMC effect [34] might be taken as an evidence of quark delocalization), it has far-reaching implications however. The phase transition from nuclear matter to quark-gluon plasma would be at best a second order one or just a crossover as happened in the transition from atomic gases into plasma and would make the already hard identification of this phase transition even harder [2].  $d^*$  search is a critical test of the quark delocalization mechanism.

## II. ELECTRO-PRODUCTION MECHANISM OF $D^*$

$d^*$  is a spin 3 state. Its dominant hadronic component is  $\Delta\Delta$ . To produce a  $d^*$  from a nuclear target, one has to change two nucleons into two  $\Delta$ 's. A virtual photon exchange can only excite one nucleon into a  $\Delta$ . Double photon exchange is a fourth order QED process. Its contribution to the cross section will be proportional to  $\alpha^4$ , a too small effect. Here  $\alpha = e^2/(\hbar c)$ . Therefore the electro- production of  $d^*$  is critically dependent on the gluon exchange current in the quark-gluon description and on the meson exchange current in the hadronic description. The gluon exchange current is unique as depicted in Fig.1.

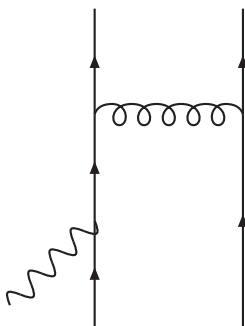


FIG. 1. Quark gluon exchange current

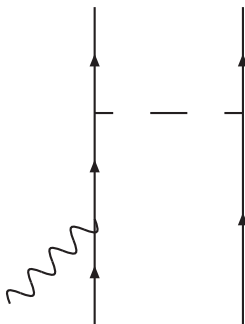


FIG. 2. Quark meson exchange current

However as mentioned before that some models emphasized the Goldstone boson quark coupling. Then there will be meson exchange current as depicted in Fig.2 even within a baryon. This makes the exchange current in the quark-gluon description rather model dependent. J.A.Gomez Tejedor and E. Oset(GO) calculated the  $ed \rightarrow e'p\Delta$  and  $\gamma d \rightarrow \Delta\Delta \rightarrow pn\pi^+\pi^-$  cross sections with the hadronic degree of freedom [35]. This approach is complicated by the many effective meson-baryon couplings. However those coupling constants have been fixed by the experimental data. We will take GO approach to do the  $d^*$  electro-production cross section calculation. Based on the isospin and angular momentum conservation and taking into account the results of GO, the following Feynman diagrams are included in our calculation,

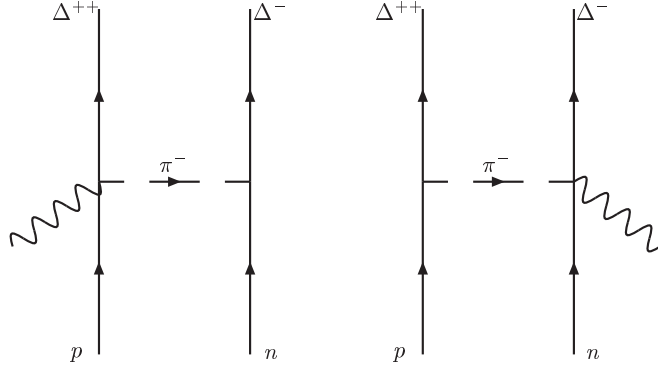


FIG. 3. Kroll-Ruderman process

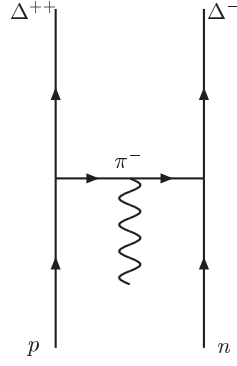


FIG. 4. Meson exchange current

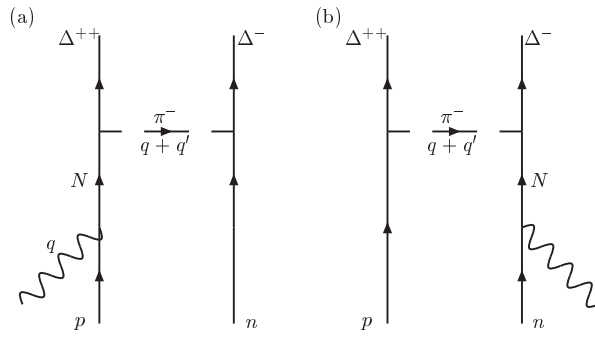


FIG. 5.  $NN$  intermediate state

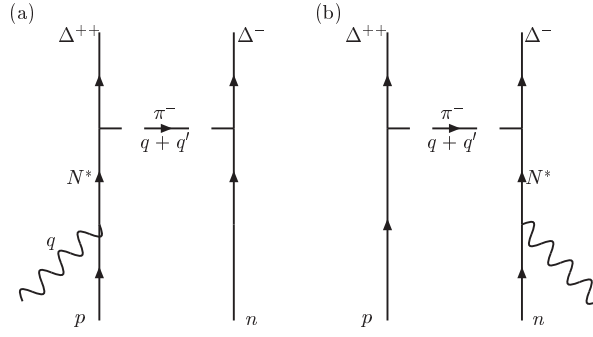


FIG. 6.  $NN^*$  intermediate state

The  $d^*$  is an isospin  $I=0$  state,

$$|d^*\rangle = \frac{1}{2}(\Delta^{++}\Delta^- - \Delta^+\Delta^0 + \Delta^0\Delta^+ - \Delta^-\Delta^{++}). \quad (1)$$

The Kroll-Ruderman term Fig.3 does not contribute due to the cancellation of the  $\pi^+$  and  $\pi^-$  exchange between different components of  $d^*$  and  $d$ . The meson exchange term Fig.4. does not contribute for the same reason. Therefore only Fig.5 and 6 contribute to the  $d^*$  production.

For the  $NN^*$  intermediate state, only  $N^*(1520) IJ^P = \frac{1}{2}\frac{3}{2}^+$  has been included. Because the results of GO [35] show that the contribution of  $NN^*(1520)$  might be more important, the  $NN^*(1440)$  term will be left for further refinement. The  $\Delta\Delta$  and the D-wave components of deuteron are neglected temporary.

### III. MESON EXCHANGE CURRENT AND CROSS SECTION

The general electron scattering cross section formula of Donnelly and Raskin [36] will be used to calculate the inelastic  $d^*$  production.

$$\frac{d\sigma}{d\Omega} = \sigma_M(\nu_L R_{fi}^L + \nu_T R_{fi}^T + \nu_{TT} R_{fi}^{TT} + \nu_{TL} R_{fi}^{TL}) f_{rec}^{-1}, \quad (2)$$

where  $\sigma_M$  is the Mott scattering cross section,

$$\sigma_M = \left( \frac{\alpha \cos \frac{\theta_e}{2}}{2\epsilon \sin^2 \frac{\theta_e}{2}} \right)^2, \quad (3)$$

$$\nu_L = \left( \frac{q^2}{\vec{q}^2} \right)^2, \quad (4)$$

$$\nu_T = -\frac{1}{2} \left( \frac{q^2}{\vec{q}^2} \right) + \tan^2 \frac{\theta_e}{2}, \quad (5)$$

$$\nu_{TT} = -\frac{1}{2} \left( \frac{q^2}{\vec{q}^2} \right), \quad (6)$$

$$\nu_{TL} = \frac{1}{\sqrt{2}} \left( \frac{q^2}{\vec{q}^2} \right) \sqrt{-\left( \frac{q^2}{\vec{q}^2} \right) + \tan^2 \frac{\theta_e}{2}}, \quad (7)$$

$$R_{fi}^L = |\rho(\vec{q})_{fi}|^2, \quad (8)$$

$$R_{fi}^T = |J(\vec{q}, +1)_{fi}|^2 + |J(\vec{q}, -1)_{fi}|^2, \quad (9)$$

$$R_{fi}^{TT} = 2\text{Re}\{J^*(\vec{q}, +1)_{fi} J(\vec{q}, -1)_{fi}\}, \quad (10)$$

$$R_{fi}^{TL} = -2\text{Re}\{\rho^*(\vec{q})_{fi}(J(\vec{q}, +1)_{fi} - J(\vec{q}, -1)_{fi})\}, \quad (11)$$

$$f_{rec} = 1 + \frac{2\epsilon}{M_T} \sin^2 \frac{\theta_e}{2}. \quad (12)$$

$f_{rec}$  is the recoil correction. The four vector current  $J^\mu(\vec{q})_{fi}$  is the Fourier transformed four vector transition current of the target,

$$J^\mu(\vec{q})_{fi} = \int d^3\vec{r} e^{i\vec{q}\cdot\vec{r}} \langle f | J^\mu(\vec{r}) | i \rangle, \quad (13)$$

$$\vec{J}(\vec{q})_{fi} = \sum_{m=0,\pm 1} J(\vec{q}, m) \vec{e}(\vec{q}; 1, m), \quad (14)$$

$$\vec{e}(\vec{q}; 1, 0) = \vec{u}_z, \quad \vec{e}(\vec{q}; 1, \pm 1) = \mp \frac{1}{\sqrt{2}} (\vec{u}_x \pm i\vec{u}_y), \quad (15)$$

$$\vec{u}_x = -\frac{\vec{q} \times (\vec{k} \times \vec{k}')}{|\vec{q} \times (\vec{k} \times \vec{k}')|}, \quad \vec{u}_y = \frac{\vec{k} \times \vec{k}'}{|\vec{k} \times \vec{k}'|}, \quad \vec{u}_z = \frac{\vec{q}}{|\vec{q}|}, \quad (16)$$

$$\rho(\vec{q})_{fi} = \frac{|\vec{q}|}{\omega} J(\vec{q}, 0)_{fi}. \quad (17)$$

The last Eq. is obtained from the four vector current conservation.  $q$ ,  $k$ , and  $k'$  are the four momentum transfer, the initial and final momentum of the scattered electron depicted in Fig.7.  $q = k - k'$ .  $\theta_e$  is the electron scattering angle in the lab system.  $M_T$  is the mass of the target, mass of deuteron in our case.  $\epsilon$  ( $\epsilon'$ ) is the initial(final) energy of the scattered electron, and  $\omega = \epsilon - \epsilon'$ .

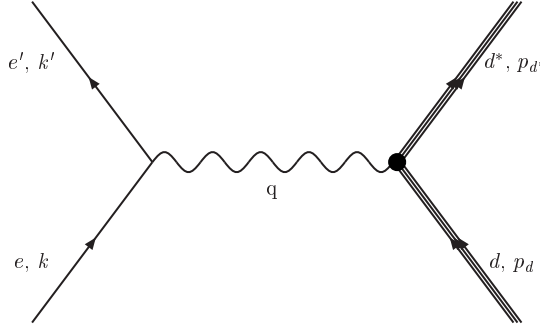


FIG. 7. The electron-deuteron inelastic scattering

For the unpolarized electron scattering, the cross terms  $R_{fi}^{TT}$  and  $R_{fi}^{TL}$  do not contribute. The angular momentum and parity conservation ( $IJ^P = 01^+$  for  $d$  and  $03^+$  for  $d^*$ ) restrict the multipole moments further. Only the following 5 multipole moments contribute to the  $ed \rightarrow ed^*$  process:

$$F_2^C(|\vec{q}|) = \sqrt{\frac{4\pi}{3}} \langle 3 \| M_2(|\vec{q}|) \| 1 \rangle, \quad (18)$$

$$F_2^E(|\vec{q}|) = \sqrt{\frac{4\pi}{3}} \langle 3 \| T_2^E(|\vec{q}|) \| 1 \rangle, \quad (19)$$

$$F_3^M(|\vec{q}|) = \sqrt{\frac{4\pi}{3}} \langle 3 \| iT_3^M(|\vec{q}|) \| 1 \rangle, \quad (20)$$

$$F_4^C(|\vec{q}|) = \sqrt{\frac{4\pi}{3}} \langle 3 \| M_4(|\vec{q}|) \| 1 \rangle, \quad (21)$$

$$F_4^E(|\vec{q}|) = \sqrt{\frac{4\pi}{3}} \langle 3 \| T_4^E(|\vec{q}|) \| 1 \rangle. \quad (22)$$

The multipole moments are defined through the following multipole expansion,

$$J(\vec{q}, 0)_{fi} = \frac{\omega}{|\vec{q}|} \sqrt{4\pi} \sum_{J \geq 0} \sqrt{2J+1} i^J \langle f | M_{J0}(|\vec{q}|) | i \rangle, \quad (23)$$

$$J(\vec{q}, \pm 1)_{fi} = -\sqrt{2\pi} \sum_{J \geq 0} \sqrt{2J+1} i^J \left( \langle f | T_{J,\pm 1}^e(|\vec{q}|) | i \rangle \pm \langle f | T_{J,\pm 1}^m(|\vec{q}|) | i \rangle \right), \quad (24)$$

$$M_{Jm}(|\vec{q}|) = \int d^3\vec{r} M_{Jm}(|\vec{q}|\vec{r}) \rho(\vec{r}), \quad (25)$$

$$T_{Jm}^E(|\vec{q}|) = \int d^3\vec{r} \frac{1}{|\vec{q}|} (\nabla \times M_{JLm}(|\vec{q}|\vec{r})) \cdot \vec{J}(\vec{r}), \quad (26)$$

$$T_{Jm}^M(|\vec{q}|) = \int d^3\vec{r} M_{JLm}(|\vec{q}|\vec{r}) \cdot \vec{J}(\vec{r}), \quad (27)$$

$$M_{Jm}(|\vec{q}|\vec{r}) = j_J(|\vec{q}|r) Y_{Jm}(\hat{r}), \quad (28)$$

$$M_{JLm}(|\vec{q}|\vec{r}) = j_J(|\vec{q}|r) Y_{JLm}(\hat{r}), \quad (29)$$

$$Y_{JLm}(\vec{r}) = [Y_L(\hat{r}) \otimes e(\vec{q}; 1)]_{JM}. \quad (30)$$

The transition current resulted from Fig.5(a) is

$$\begin{aligned} \rho(\vec{q}) &= e F^N(q^2) \frac{M_N}{E(p)} \frac{1}{p^0 - E(p) + i\epsilon} \left( \frac{f^*}{\mu} \right)^2 \vec{S}_1^\dagger \cdot (\vec{q} + \vec{q}') \vec{S}_2^\dagger \cdot (\vec{q} + \vec{q}') \\ &F_\pi^2 \left( (q + q')^2 \right) \frac{1}{(q + q')^2 - \mu^2 + i\epsilon} T_1^\dagger \cdot T_2^\dagger \delta^3(\vec{q} + \vec{p}_d - \vec{p}_{d*}), \end{aligned} \quad (31)$$

$$\begin{aligned} \vec{J}(\vec{q}) &= e \left\{ F^N(q^2) \frac{\vec{p}_1 + \vec{p}}{2M_N} + \frac{i}{2M_N} \vec{\sigma} \times \vec{q} G_m^N(q^2) \right\} \frac{M_N}{E(p)} \frac{1}{p^0 - E(p) + i\epsilon} \left( \frac{f^*}{\mu} \right)^2 \\ &\vec{S}_1^\dagger \cdot (\vec{q} + \vec{q}') \vec{S}_2^\dagger \cdot (\vec{q} + \vec{q}') F_\pi^2 \left( (q + q')^2 \right) \frac{1}{(q + q')^2 - \mu^2 + i\epsilon} T_1^\dagger \cdot T_2^\dagger \delta^3(\vec{q} + \vec{p}_d - \vec{p}_{d*}). \end{aligned} \quad (32)$$

A similar transition current resulted from Fig.6(a) is

$$\begin{aligned} \rho(\vec{q}) &= (\tilde{g}_\gamma - \tilde{g}_\sigma) \frac{\vec{S}_1^\dagger \cdot \vec{q}}{M_{N^*} - M_N} \tilde{f}_{N^* \Delta \pi} \frac{1}{\sqrt{S} - M_{N^*} + i \frac{\Gamma(\sqrt{S})}{2}} \left( -\frac{f^*}{\mu} \right) \\ &F_\pi^2 \left( (q + q')^2 \right) \frac{\vec{S}_2^\dagger \cdot (\vec{q} + \vec{q}')}{(q + q')^2 - \mu^2 + i\epsilon} T_1^\dagger \cdot T_2^\dagger \delta^3(\vec{q} + \vec{p}_d - \vec{p}_{d*}), \end{aligned} \quad (33)$$

$$\begin{aligned} \vec{J}(\vec{q}) &= (\tilde{g}_\gamma - \tilde{g}_\sigma) \vec{S}_1^\dagger \tilde{f}_{N^* \Delta \pi} \frac{1}{\sqrt{S} - M_{N^*} + i \frac{\Gamma(\sqrt{S})}{2}} \left( -\frac{f^*}{\mu} \right) \\ &F_\pi^2 \left( (q + q')^2 \right) \frac{\vec{S}_2^\dagger \cdot (\vec{q} + \vec{q}')}{(q + q')^2 - \mu^2 + i\epsilon} T_1^\dagger \cdot T_2^\dagger \delta^3(\vec{q} + \vec{p}_d - \vec{p}_{d*}). \end{aligned} \quad (34)$$

Fig.5(b) and Fig.6(b) will give similar transition currents.

In obtaining these transition currents, the following effective Lagrangian have been used,

$$L_{NN\gamma} = -e \bar{\Psi}_N \left( \gamma^\mu A_\mu - \frac{\chi_N}{2M_N} \sigma^{\mu\nu} \partial_\nu A_\mu \right) \Psi_N \quad (35)$$

$$L_{N\Delta\pi} = -\frac{f^*}{\mu} \Psi_\Delta^\dagger S_i^\dagger (\partial_i \phi^\lambda) T^{\lambda\dagger} \Psi_N + h.c. \quad (36)$$

$$L_{NN^*\gamma} = \bar{\Psi}_{N^*} \left[ \tilde{g}_\gamma \vec{S}^\dagger \vec{A} - i \tilde{g}_\sigma (\vec{S}^\dagger \times \vec{\sigma}) \vec{A} \right] \Psi_N + h.c. \quad (37)$$

$$L_{N^*\Delta\pi} = i \bar{\Psi}_{N^*} \tilde{f}_{N^*\Delta\pi} \phi^\lambda T^{\lambda\dagger} \Psi_\Delta + h.c. \quad (38)$$

In these expressions  $\Phi$ ,  $\Psi_N$ ,  $\Psi_\Delta$ ,  $\Psi_{N^*}$ , and  $A_\mu$  stand for the pion, nucleon,  $\Delta$ ,  $N^*(1520)$ , and photon fields respectively;  $M_N$  and  $\mu$  are the nucleon and pion masses;  $\vec{\sigma}$  and  $\vec{\tau}$  are the usual  $\frac{1}{2}$  spin and isospin Pauli operators;  $\vec{S}^\dagger$  and  $\vec{T}^\dagger$  are the transition spin and isospin operators from  $\frac{1}{2}$  to  $\frac{3}{2}$  with the normalization,

$$\langle \frac{3}{2}, M | S_\nu^\dagger | \frac{1}{2}, m \rangle = C \left( \frac{1}{2}, 1, \frac{3}{2}; m, \nu, M \right) \quad (39)$$

All the effective coupling constants, form factors, and the propagators are taken from GO [35]. They are copied here to make this report self contained and can be read without further check of many references.

$$\chi^N = \begin{Bmatrix} 1.79 & \text{proton} \\ -1.91 & \text{neutron} \end{Bmatrix}$$

$$f^* = 2.13 \quad \tilde{f}_{N^* \Delta \pi} = 0.677$$

$$\tilde{g}_\gamma = \begin{Bmatrix} 0.108 & \text{proton} \\ -0.129 & \text{neutron} \end{Bmatrix} \quad \tilde{g}_\sigma = \begin{Bmatrix} -0.049 & \text{proton} \\ -0.0073 & \text{neutron} \end{Bmatrix}$$

For the nucleon propagator, only the positive energy part is retained where  $E(p) = \sqrt{M_N^2 + p^2}$ ; for the  $N^*$ , the finite width  $\Gamma$  has been included where

$$S = p^{02} - p^2, \quad \Gamma(\sqrt{S}) = \Gamma(M_N^*) q_{cm}^5(\sqrt{S}) / q_{cm}^5(M_N^*). \quad (40)$$

The form factors are taken from GO [35] to keep the model consistent.

$$F_\pi(q^2) = \frac{\Lambda_\pi^2 - m_\pi^2}{\Lambda_\pi^2 - q^2}; \quad \Lambda_\pi \sim 1250 \text{ MeV} \quad (41)$$

Sachs's form factors are given by

$$G_M^N(q^2) = \frac{\mu_N}{(1 - \frac{q^2}{\Lambda^2})^2}; \quad G_E^N(q^2) = \frac{1}{(1 - \frac{q^2}{\Lambda^2})^2} \quad (42)$$

with  $\Lambda^2 = 0.71 \text{ GeV}^2$ ;  $\mu_p = 2.793$ ;  $\mu_n = -1.913$ .

The relation between  $F_1^p(q^2)$  (Dirac's form factor) and  $G_E^p(q^2)$  is :

$$F_1^p(q^2) = G_E^p(q^2) \frac{(1 - \frac{q^2 \mu_p}{4m_N^2})}{(1 - \frac{q^2}{4m_N^2})} \quad (43)$$

and  $F_1^n = 0$ .

To calculate the hadronic  $d \rightarrow d^*$  transition current, a single Gaussian wave function with a size parameter  $b^* = 0.7 \text{ fm}$  is used to approximate the  $d^*$  internal motion. For the deuteron  $d$  a three Gaussian fitted to the ground state properties has been used, three size parameters are  $b = (4.0975, 1.8252, 0.8837) \text{ fm}$  with normalization coefficient  $c = (0.31491, 0.49716, 0.36926)$ . [2] The  $d^*$  mass is taken to be 2.1 GeV. Due to the special spin(1 for  $d$  and 3 for  $d^*$ ) and orbital angular momentum(both 0) internal structure and the spin property of the meson exchange current, only  $F_2^C$ ,  $F_2^E$  and  $F_3^M$  three transition form factors remain after the integration over the internal spin and orbital variables of  $d$  and  $d^*$ . Fig.5 contributes one  $F_2^C$ , one  $F_3^M$  and two  $F_2^E$  (from convective and magnetic current respectively), Fig.6 contributes one  $F_2^C$  and one  $F_2^E$  term.

#### IV. RESULTS AND DISCUSSIONS

The calculated  $d^*$  electro production cross sections are shown in Fig.8 . The four curves correspond to four electron energies 0.8, 1.0, 1.2 and 1.5 GeV. The shape of the differential cross section is dominated by the Mott cross section but modulated by the inelastic transition form factors. The value around 30 degree in the laboratory frame is about 10 nb for 1 GeV electron. In Fig.9, 10 and 11, the transition form factors  $F_2^C$ ,  $F_2^E$  and  $F_3^M$  are shown. The dashed curves correspond to the contribution of  $NN$  intermediate state while the full curves correspond to the sum of contributions of two intermediate states. The  $NN$  intermediate state is the dominant one except at large angles, where the  $NN^*$



contribution is more important. Fig.12 shows the differential cross section due to the  $NN$  intermediate state only as well as a comparison to the full one.

The produced  $d^*$  will decay into  $NN$  and  $NN\pi$ . The cross section, 10 nb around 30 degree for 1 GeV electron, is about two order smaller than that of quasi elastic  $ed \rightarrow e'NN$  and  $\Delta$  resonance production  $ed \rightarrow e'N\Delta \rightarrow e'NN\pi$  processes. Therefore the normal measurement of the inelastic electron scattering can not find the signal of  $d^*$  even it is existed, i.e., the  $d^*$  signal will be buried in the quasi elastic or  $\Delta$  resonance background. A special kinematics and detector system must be studied further both theoretically and experimentally in order to pin down the weak signal of  $d^*$  resonance from the strong background.

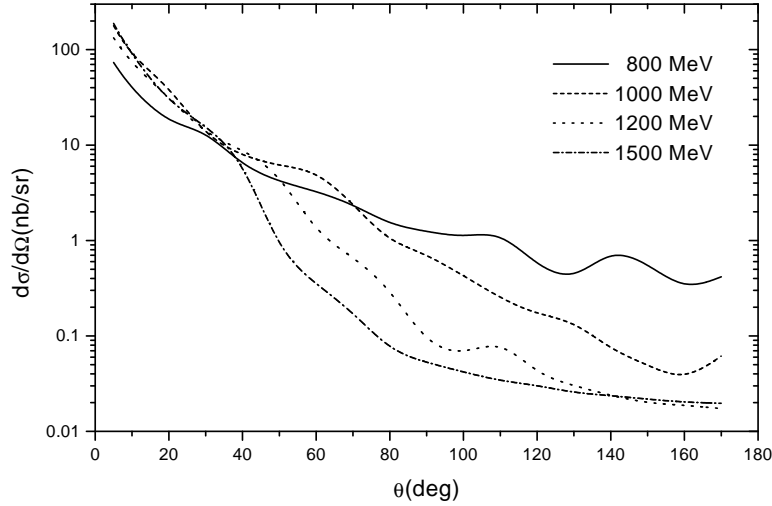


FIG. 8.  $ed \rightarrow ed^*$  differential cross sections

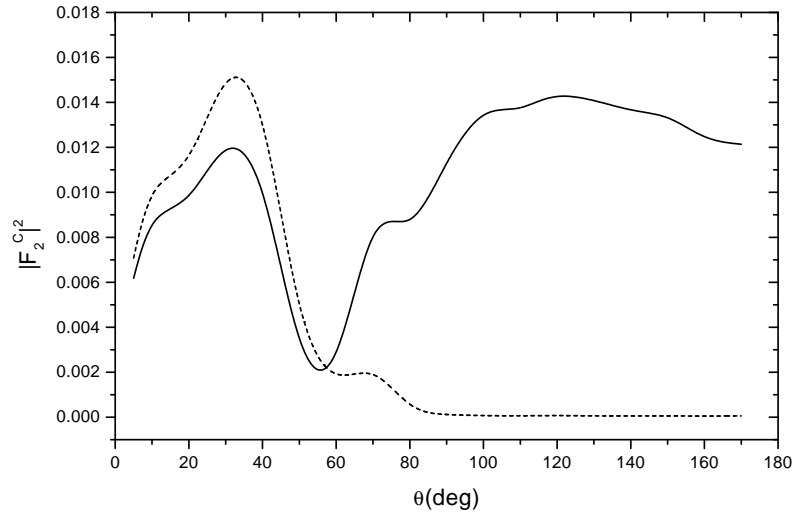


FIG. 9.  $d \rightarrow d^*$  transition form factors:  $|F_2^C|^2$ ,  $k_0 = 1.5 \text{ GeV}$ , the dashed curve corresponds to the  $NN$  intermediate state contribution, the full curve corresponds to the sum of  $NN$  and  $NN^*$  intermediate state contributions.

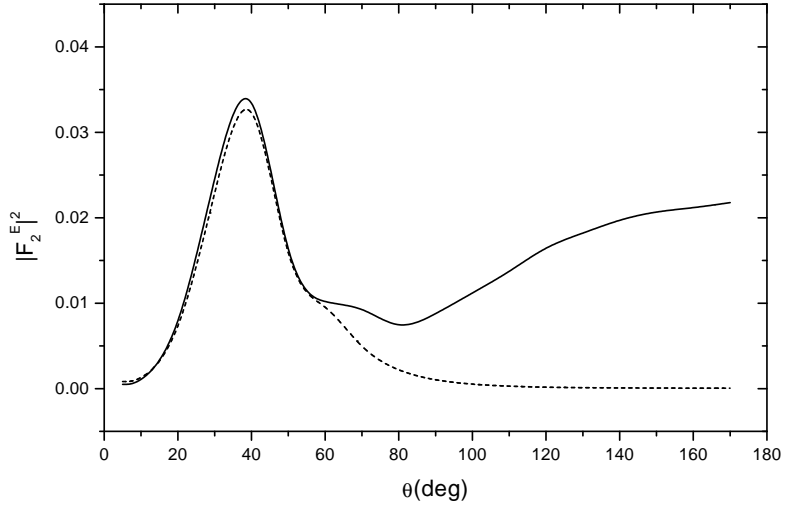


FIG. 10. Same as FIG. 9 for  $|F_2^E|^2$

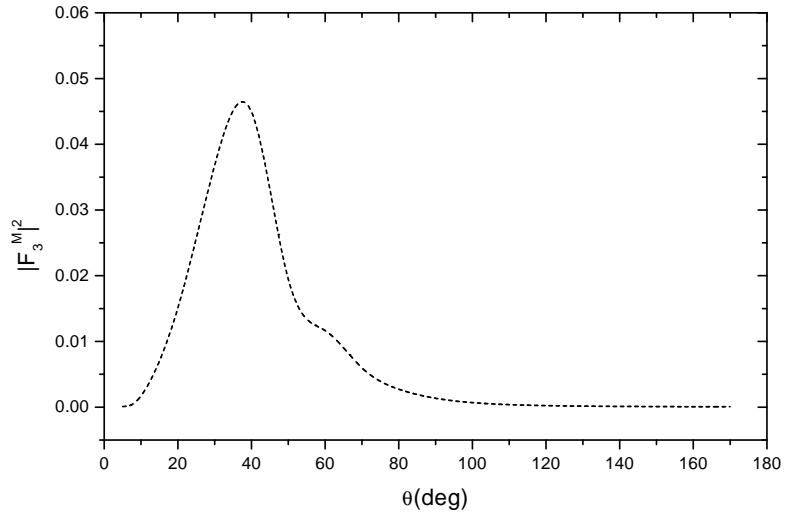


FIG. 11. Same as FIG. 9 for  $|F_3^M|^2$

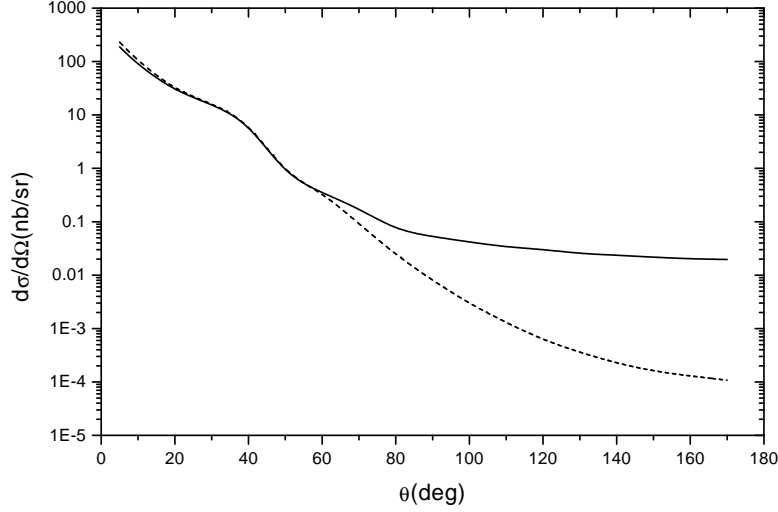


FIG. 12. Same as FIG. 9 for differential cross sections  $d\sigma/d\Omega$

In our model calculation, some simplifications have been assumed. The D wave component of deuteron has been neglected. Even though it is a small component, its contribution to the  $d^*$  production might not be small enough to be neglected, because only a recoupling of spin and orbital angular momentum will be able to transit the deuteron  $^3D_1$  into a  $^3D_3$  NN component of  $d^*$ . The initial state correlation, i.e., the  $\Delta - \Delta$  component of deuteron is an even smaller component, but only a spin recoupling is needed to transit it into  $d^*$ , therefore its contribution should be checked as well.  $d^*$  is a six quark state [3] rather than a  $\Delta - \Delta$  bound state. To model it as a pure two  $\Delta$  bound state and use a single Gaussian wave function to describe its internal structure will overestimate the calculated cross section. The contribution of  $NN^*(1440)$  intermediate state should be added especially in the large angle part. Due to these approximations the calculated cross section is an estimate of the  $d^*$  electro production. On the other hand all of the above mentioned corrections are minor effects, the order(10 nb around 30 degree for 1 GeV electron) obtained from this calculation might be stable against these fine tunes. Further calculation is going on, especially a quark model calculation is also doing to check if a single Gaussian approximation of the  $d^*$  internal wave function has overestimated the cross section.. The results will be reported later.

The electro production of  $d'$  dibaryon is being measured. This calculation can be extended to that process and will be a good check not only of the electro production model used here but also of the  $d'$  dibaryon analysis itself.

Very helpful discussions with C.W. Wong, T. Goldman and Stan Yen are acknowledged. We are also greatly indebted to J.A. Gómez Tejedor and E. Oset for their helpful private communications.

This research is supported by NSF, SSTD and the post Dr. foundation of SED of China. Part of the numerical calculation is done on the SGI Origin 2000 in the lab of computational condensed matter physics.

- 
- [1] T. Goldman, K. Maltman, G.J. Stephenson, Jr., K.E. Schmidt, and F. Wang, Phys. Rev. **C39**, 1889 (1989).
  - [2] C. W. Wong, Phys. Rev. **C57**, 1962 (1998).
  - [3] F. Wang, G.H. Wu, L.J. Teng, and T. Goldman, Phys. Rev. Lett. **69**, 2901 (1992). F. Wang, J.L. Ping, G.H. Wu, L.J. Teng, and T. Goldman, Phys. Rev. **C51**, 3411 (1995). T. Goldman, K. Maltman, G.T. Stephenson, Jr., J.L. Ping, and F. Wang, Mod. Phys. Lett. **A13**, 59 (1998).
  - [4] F. Lehar, in Baryons'98, eds. D.W. Menze and B.Ch. Metsch (World Scientific, Singapore, 1999) p.622.
  - [5] R. Bilger, H. Clement and M. Schepkin, Phys. Rev. Lett. **71**, 42 (1993).
  - [6] R.L. Jaffe, Phys. Rev. Lett. **38**, 195 (1977).
  - [7] H. Yukawa, Proc. Phys. Math. Soc. Jpn. **17**, 48 (1935).
  - [8] M.C.M. Rentmeester, R.G.E. Timmermans, J.L. Friar and J.J.de Swart, Phys. Rev. Lett. **82**, 4992 (1999) and references therein; C. Harzer, H. Muether and R. Machleidt, Phys. Lett. **B459**, 1 (1999).

- [9] T. Kamae and T. Fujita, Phys. Rev. Lett. **38**, 471 (1977).
- [10] S. Weinberg, Physica **96A**, 327 (1979); Phys. Lett. **B251**, 288 (1990); Nucl. Phys. **B363**, 3 (1991).
- [11] D.B. Kaplan, in Baryons'98, eds. D.W. Menze and B.Ch. Metsch (World Scientific, Singapore, 1999) p.160.
- [12] L.Ya. Glozman and D.O. Riska, Phys. Rep. **268**, 263 (1996); D.O. Riska and G.E. Brown, hep-ph/9902319.
- [13] A. Manohar and H. Georgi, Nucl. Phys. **B234**, 189 (1984).
- [14] Y. Fujiwara, C. Nakamoto and Y. Suzuki, Phys. Rev. Lett. **76**, 2242 (1996) and references there in.
- [15] M. Oka, K. Shimizu, and K. Yazaki, Phys. Lett. **B130**, 365 (1983); Nucl. Phys. **A464**, 700 (1987); M. Oka, Phys. Rev. **D38**, 298 (1988); A. Faessler and U. Straub, Phys. Lett. **B183**, 10 (1987).
- [16] A. De Rujula, H. Georgi and S.L. Glashow, Phys. Rev. **D12**, 147 (1975).
- [17] N. Isgur and G. Karl, Phys. Rev. **D18**, 4187 (1978); **D19**, 2653 (1979); **D20**, 1191 (1979).
- [18] C.W. Wong, Phys. Rep. **136**, 1 (1986) and references therein.
- [19] A. Chodos, R.L. Jaffe, K. Johnson, C.B. Thorn and V. Weisskopf, Phys. Rev. **D9**, 3471 (1974).
- [20] P.J.G. Mulders, A.T.M. Aerts, and J.J. de Swart, Phys. Rev. **D17**, 260 (1978).
- [21] N. Isgur, in Hadrons and Hadronic Matter, eds. D. Vautherin et al. (Plenum Press, New York, 1990) p.21
- [22] R.L. Jaffe and F.E. Low, Phys. Rev. **D19**, 2105 (1979); E.L. Lomon, Phys. Rev. **D26**, 576 (1982); P. LaFrance and E.L. Lomon, Phys. Rev. **D34**, 1341 (1986).
- [23] Yu.A. Simonov, Phys. Lett. **B107**, 1 (1981); Sov. J. Nucl. Phys. **36**, 422 (1982).
- [24] T.H.R. Skyrme, Nucl. Phys. **31**, 556 (1962); E. Witten, Nucl. Phys. **B160**, 57 (1979).
- [25] T.S. Walhout and J. Wambach, Phys. Rev. Lett. **67**, 314 (1991); N.R. Walet and R.D. Amado, Phys. Rev. Lett. **68**, 3849 (1992).
- [26] R.L. Jaffe and C.L. Korpa, Nucl. Phys. **B258**, 468 (1985).
- [27] G.H. Wu, L.J. Teng, J.L. Ping, F. Wang and T. Goldman, Mod. Phys. Lett. **A10**, 1895 (1995); Phys. Rev. **C53**, 1161 (1996).
- [28] T. Goldman, K. Maltman, G.J. Stephenson, Jr. and K.E. Schmidt, Nucl. Phys. **A481**, 621 (1988); Phys. Lett. **B324**, 1 (1994).
- [29] J.L. Ping, F. Wang and T. Goldman, Nucl. Phys. **A657**, 95 (1999); G.H. Wu, J.L. Ping, L.J. Teng, F. Wang and T. Goldman, LANL preprint LA-UR-98-5841, hep-ph/9812079.
- [30] X.Q. Yuan et al., Commun. Theor. Phys. **32**, 169 (1999).
- [31] M. Oka and K. Yazaki, in Quarks and Nuclei, ed. W. Weise (World Scientific, Singapore, 1984) p.489.
- [32] R. Walet, Phys. Rev. **C48**, 2222 (1993).
- [33] US NSAC Long Range Plan URL: <http://pubweb.bnl.gov/~nsac>
- [34] F.E. Close, R.L. Jaffe, R.G. Roberts and G.G. Ross, Phys. Rev. **D31**, 1004 (1985).
- [35] J. A. Gómez Tejedor and E. Oset, Nucl. Phys. **C571**, 667 (1994); **A580**, 577 (1994); **A600**, 413 (1996); J.A. Gómez Tejedor, E. Oset and H. Toki, Phys. Lett. **B346**, 240 (1995); J. C. Nacher and E. Oset, nucl-th/9804006.
- [36] T.W. Donnelly and A.S. Raskin, Ann. Phys. **169**, 287 (1986).